



Published in final edited form as:

J Vasc Surg. 2016 August ; 64(2): 484–493. doi:10.1016/j.jvs.2015.01.031.

Effect of DNase-I Treatment and Neutrophil Depletion on Acute Limb Ischemia Reperfusion Injury in Mice

Hassan Albadawi^{1,2,*}, Rahmi Oklu^{1,3,*}, Rita Elise Raacke Malley², Ryan M O'Keefe², Thuy P. Uong², Nicholas R Cormier², and Michael T. Watkins^{1,2}

¹Harvard Medical School, Boston, Massachusetts

²Department of Surgery, Division of Vascular and Endovascular Surgery, Massachusetts General Hospital, Boston, Massachusetts

³Department of Radiology, Division of Vascular Imaging and Intervention, Massachusetts General Hospital, Boston, Massachusetts

Abstract

Objective—Extracellular traps-(ETs) consist of DNA-protein-complexes formed following tissue injury contributes to the inflammatory and thrombosis cascades thereby exacerbating injury. Exogenous DNase-1 has been suggested as a therapeutic strategy to limit injury in the brain and myocardium.. These studies were designed to evaluate the effects of exogenous DNase-I treatment on skeletal muscle injury following acute hind limb ischemia-reperfusion (IR) injury in mice, and to determine whether neutrophils were a major source of ETs in postischemic muscle tissue.

Methods—C57BL6 mice were subjected to 1.5 hrs tourniquet ischemia and 24 hrs reperfusion with and without human recombinant DNase-I treatment. A separate set of mice was subjected to neutrophil depletion, followed by the same intervals of IR. Laser Doppler imaging and tissue harvesting was done at 24 hrs for assessment of limb perfusion, muscle fiber injury, ATP, markers of inflammation, thrombosis, and ETs formation.

Results—DNase-I treatment significantly reduced ETs detection in post-ischemic muscle but did not alter skeletal muscle fiber injury, levels of pro-inflammatory molecules or ATP. DNase-I treatment did enhance postischemic hind limb perfusion, decreased infiltrating inflammatory cells and reduced the expression of Thrombin-Anti-Thrombin-III. Neutrophil depletion resulted in a significant yet small reduction in ETs in the post ischemic muscle. Neutrophil depletion did not alter skeletal muscle fiber injury, hind limb perfusion, or ATP levels.

Correspondence to: Hassan Albadawi, MD, Vascular Research Laboratory, Department of Surgery, Division of Vascular and Endovascular Surgery, Massachusetts General Hospital, 70 Blossom Street-Edwards 301, Boston, MA 02114.
halbadawi@partners.org, Phone: 617-724-7818, Fax: 617-726-2560.

*These authors contributed equally to this work

This work was presented at the scientific program of the academic surgical congress on February 6, 2014 in San Diego California as a quick shot oral presentation.

Publisher's Disclaimer: This is a PDF file of an unedited manuscript that has been accepted for publication. As a service to our customers we are providing this early version of the manuscript. The manuscript will undergo copyediting, typesetting, and review of the resulting proof before it is published in its final citable form. Please note that during the production process errors may be discovered which could affect the content, and all legal disclaimers that apply to the journal pertain.

Conclusions—These data suggest that neither DNase-I treatment nor Neutrophil depletion were protective against IR injury, even though both decreased ETs detection in skeletal muscle following IR. Neutrophils are not the only source of ETs following IR.

Introduction

Acute lower-limb ischemia-reperfusion injury (IR) is a common occurrence following revascularization. Pathologically, acute IR is comprised of tissue edema, muscle necrosis, inflammation, and thrombosis. Inflammation resulting from IR injury incites tissue granulocyte infiltration. Recent studies have shown that activated neutrophils following ischemic injury can lead to release of neutrophil extracellular traps (ETs)¹⁻⁴. ETs are naturally degraded by nucleases such as DNase-I. Pulmozyme, which is a commercially available recombinant human DNase-I approved for the treatment of cystic fibrosis⁵, has been used in multiple animal studies investigating ETs. These studies have involved thrombosis animal models as well as human venous thrombosis and vascular diseases⁶⁻¹². In addition, there have been reports associating ET fragments i.e., circulating genomic DNA, and coronary artery disease, prothrombotic state, and occurrence of adverse cardiac events¹³. Studies in venous thrombosis have suggested that ETs create scaffold structures providing stability to the acute fibrin-rich thrombus inside the vascular bed and enhancing its transformation to collagen rich chronic thrombus. Furthermore, experimental models of ischemic injury in cardiac and brain tissues have also established a role for ETs in promoting thrombosis or exacerbating tissue injury while Pulmozyme treatment aimed at degrading extracellular DNA was reported to have rescue effects^{2, 14}. ET formation in skeletal muscle tissue following acute hind limb IR has also been recently described¹. Studies suggested that ETs participate in the acute inflammatory and thrombosis response inside the microenvironment of the injured tissue thereby exacerbating tissue injury. While ET detection following IR was presumed to be derived from neutrophils, it is unknown whether ETs are associated with muscle fiber injury and whether strategies targeting or depleting ETs will lead to alleviation of muscle fiber injury. It is also known that the presence of γ -Actin, a naturally occurring inhibitor of DNase-I^{15, 16}, is enhanced after IR.

The purpose of these experiments was to determine whether the administration of Pulmozyme confers protection against skeletal muscle fiber injury, and enhances perfusion and reduces tissue inflammation and thrombosis in a mouse model of acute hind limb IR. In addition we investigated whether granulocyte depletion, which is considered a major source of ET release, will reduce ET formation and ameliorate skeletal muscle injury following IR.

Material and Methods

Acute hind limb ischemia reperfusion and treatment protocols

Two sets of C57BL6 male mice were subjected to 1.5 hrs of unilateral hind limb tourniquet ischemia followed by 24 hrs reperfusion (IR) as previously described¹⁷. In brief, ischemia was induced by applying a calibrated orthodontic rubber band for 1.5 hrs, which was confirmed by laser Doppler imaging scanner (LDI) and reperfusion was initiated by cutting the rubber band. In the first set of experiments was designated for DNase-I treatment where mice were divided into two groups (Figure-1A). The first group of mice (DNase-I, n=8)

received 50µg of human recombinant DNase-I (Pulmozyme, Genentech, San Francisco, CA) in 250µl carrier buffer intraperitoneally at 5 min before reperfusion and a second dose of 10µg intravenously at 10 min after reperfusion and a third dose of 50µg intraperitoneally at 12 hrs after reperfusion (DNase-I n=8)¹⁴. A second group of mice were subjected to the same period of IR, received similar volumes of carrier buffer alone at the same time points representing the treatment control (Control, n=8). A separate group of mice subjected to anesthesia alone was used as sham. The second set of experiments was designated for neutrophil depletion (Figure-1B). In this part of the study, two separate groups of mice received daily injections of either a rabbit anti-mouse neutrophil serum (Accurate Chemical & Scientific Co, Westbury, NY) intraperitoneally to achieve neutrophil depletion (ND; n=8), or normal rabbit serum (NS; n=7) for 48 hrs. Mice were then subjected to the same IR injury as the previous set. Both groups received additional rabbit anti-mouse serum or normal serum immediately (1 min) after the start of reperfusion. In all groups, hind limb perfusion was documented with a laser Doppler imaging, then mice were euthanized and hind limb muscle tissues were subsequently harvested for further analysis.

Quantitative assessment of skeletal muscle fiber injury

To determine the effect of DNase-I treatment on muscle fiber injury at 24 hrs reperfusion, the tibialis anterior (TA) muscles were harvested and fixed then dehydrated and imbedded in JB-4 acrylic (Polysciences Inc, Warrington, PA). 2µm thick cross sections were obtained and stained with Mason's trichrome. Randomized digital images were generated at 200x magnification.. Analysis of skeletal muscle fiber injury was performed by a blinded observer using the full-frame counting method as previously established¹⁸. Myofibers were scores and segregated into two groups; injured or uninjured based on the morphology of each individual fiber. The injury score was expressed as a percentage of the total scored myofiber per muscle as previously described^{18, 19}.

Muscle Adenosine Triphosphate (ATP) Quantification

ATP levels were measured using the ATPlite luminescence assay (PerkinElmer Life, Boston, MA) following the manufacturer's instructions as previously described¹⁹. ATP levels were expressed as nanomole per mg of protein.

Immunohistochemistry detection of inflammatory cells, Extracellular Traps and colocalization of γ -Actin with DNase-I

5µm TA muscle paraffin imbedded cross sections taken from the mid part of TA muscles were deparaffinized and rehydrated then subjected to immunohistochemistry to count the average number of infiltrating inflammatory cells by incubating the slides with rat anti-mouse Ly6B.2 as previously described¹⁹. To detect locally formed extracellular traps, tissue sections were incubated with a mouse monoclonal 0.5µg/ml of anti-histone H2A/H2B/DNA complex antibody (a gift from Dr. Marc Monestier, Temple University, PA) followed by incubation with biotinylated anti-mouse IgG (Vector Labs, Burlingame, CA) and horse radish peroxidase-conjugated Streptavidin. Specific signal was developed using cyanine-3 tyramide signal amplification reagent (Perkin Elmer, Boston, MA) according to the manufacturer's instructions. For colocalization of γ -Actin and DNase-I, tissue sections were incubated with mouse monoclonal anti γ -Actin (1:2000, Sigma) overnight at 4°C inside a

humidified chamber followed by incubation with goat anti-mouse-HRP conjugated secondary antibody (1:200, Cell Signaling) in blocking buffer for 60 minutes at room temperature. Slides were reacted for 8 minutes with TSA amplifying solution containing Cy3 fluorochrome. Slides were subsequently incubated with polyclonal rabbit anti-DNase-I IgG (Santa Cruz Biotechnology) over night followed by incubation with goat anti rabbit-Alexa-488 conjugated IgG (1:500, Invitrogen) for 1 hr at room temperature. For the negative control, the antibody was omitted and substituted with non-specific IgG. The slides were covered with mounting medium (Vectashield; Vector Labs, Burlingame, CA) and then digital images were acquired using a slide scanner (NanoZoomer2.0-RS, Hamamatsu Corporation, Middlesex, NJ) as previously described^{1, 12}. To quantify the signal derived from extracellular traps, the mean fluorescent intensity (MFI) per field was measured with Image-J software after background subtraction.

Measuring Tissue Endonuclease Activity

To verify whether DNase-I treatment enhanced local endonuclease activity; a plasmid incision assay was performed on hind limb muscle tissue extracts. Hind limb muscle tissues were extracted in a buffer containing 50 mM Tris-HCl, 0.5% Triton-X-100, 0.25 M Sucrose and 10 μ l/ml protease inhibitor cocktail (Sigma P-8340). Total protein levels were measured using a BCA protein assay (BioRad, Hercules, IL). Equal protein aliquots from each sample was added to a reaction buffer containing 1 μ g pBR322 plasmid DNA (New England Biolabs, Beverly, MA) and 2 mM CaCl₂, 5 mM MgCl₂, 10 mM Tris-HCl (pH 7.4), and 0.5 mM dithiothreitol and incubated at 37°C for 30 minutes. The reaction was stopped with a buffer containing 0.05% Bromophenol blue, 40% Sucrose, 0.1 M EDTA pH 8.0 and 1% SDS. Samples were loaded into 1% agarose gel containing 1 μ g/ml Ethidium bromide and run at 7V/cm. Digital images of the gel were acquired using FluorChem HD2 system (ProteinSimple, Santa Clara, CA) with UV light. The relative amount of endonuclease activity was calculated based on the density of the three bands for plasmid DNA present in covalently closed circular DNA (Type I), open circular DNA (Type I), or linear DNA (Type III) as was previously described^{20, 21}.

Tissue Levels of Myeloperoxidase(MPO), Keratinocyte Chemoattractant Protein(KC), and Thrombin Anti-Thrombin III Complexes (TAT III)

For quantitative assessment of local markers of inflammation we analyzed solubilized protein from the hind muscle using ELISA kit for MPO (Hycult Biotech Inc, Plymouth Meeting, PA) and KC (R&D Systems, Minneapolis, MN). To evaluate a local marker of thrombosis the levels of Thrombin-anti-thrombin Complex (TAT-III) were measured in the skeletal muscle tissue using ELISA Kit (Abcam, Cambridge, MA) as previously described¹⁹.

γ -Actin protein expression in posts ischemic skeletal muscle: solubilized protein extracts were subjected to western blotting analysis using monoclonal anti- γ -Actin IgG (1:2000, Sigma, St. Louis, MO). Specific band densities were normalized to Ponceau staining of the membrane band densities and the data was expressed as arbitrary units (AU) as was previously performed^{19, 22}.

Circulating granulocytes count

At the end of 24 hours reperfusion in the mice that received anti-Neutrophil (ND) serum or normal serum (NS), the number of circulating granulocytes was counted in whole blood using Hematology system (Heska, Loveland, CO).

Statistical Analysis

Data were expressed as mean \pm standard error of the mean and statistical analysis was performed with GraphPad Prizm version 5.2 (GraphPad Software, Inc, La Jolla, CA) using parametric or nonparametric unpaired student t test or ANOVA comparisons with a p value $<.05$ considered significant.

Results

Effect of DNase-I treatment on skeletal muscle fiber injury

Hindlimb ischemia followed by 24 hours of reperfusion in the DNase-1 treated group and in the control group resulted in marked edema and disruption of tissue architecture with sporadic fiber necrosis, hemorrhage, and infiltration of inflammatory cells (Figure-2A&B). Quantitative assessment of skeletal muscle fiber injury indicated a trend for increased fiber injury in the TA muscle of the DNase-I treated group compared to the control group, however, this observation did not reach statistical significance (Control: 20.2 ± 4.3 vs. DNase-I: 27.2 ± 2.8 , percent injured fiber per field, $P=.16$, Figure-2C).

Hind limb muscle ATP levels

To evaluate the effect of DNase-I treatment on muscle metabolic activity following IR, we measured the steady state level of ATP in the injured and the non-injured (Contralateral) muscle following IR in the DNase-I treated and control groups. In both groups, ATP levels dropped significantly in the injured limbs compared to the contralateral muscle (CM) in both groups (Control CM: 72.7 ± 11.4 vs. IR muscle: 3.54 ± 1.5 , nmol/ μ g total protein, $p<.001$) and (DNase-I CM: 75.1 ± 7.5 vs. IR muscle: 3.51 ± 0.94 , nmol/ μ g total protein, $P<.001$). However, there was no difference in the ATP levels between the contralateral or in the injured muscle from the two groups (Figure-2D).

Effect of DNase-I treatment on hind limb perfusion

Laser Doppler imaging demonstrated that DNase-I treatment helped restore hind limb perfusion (Figure-3A) compared to control (Figure-3B). Quantitative assessment of hind limb perfusion ratio (Flux ratio) between the hind limbs in each animal revealed, significantly higher hind limb perfusion ratio at 24 hrs reperfusion in the DNase-I treated mice compared to the control group (LDI Ratio: Control: 0.83 ± 0.03 vs. DNase-I: 1.03 ± 0.08 flux ratio, $P=.02$, Figure-3C). This data indicates that after treatment with DNase-I, hind limb perfusion effectively recovered to baseline levels, while untreated mice were significantly under perfused.

Local level of TAT III

The reaction of thrombin with its major inhibitor anti-thrombin III complexes (TAT-III) leads to the formation of a stable complex called (TAT-III-Complexes), which is considered a sensitive marker for the activation of the intravascular coagulation cascade. Quantitative analysis of TAT III complexes revealed that IR injury significantly increased TAT III over sham levels (Sham: 0.03 ± 0.01 vs. Control: 0.41 ± 0.05 ng/mg total protein, $p < .001$). However DNase-I treated mice had significantly lower TAT III compared to control (Control: 0.41 ± 0.05 vs. 0.28 ± 0.02 ng/mg total protein, $p < .05$, Figure-3D).

Immunohistochemical analysis of ETs levels in the hind limb muscle

Sham muscle tissue was predominantly negative for ETs staining (Figure-4A). However, mice that were subjected to ischemia and treated with carrier buffer had extensive ETs detected in the hind limb muscle at 24 hours reperfusion compared to sham muscle (Figure-4B). ETs were predominantly localized to interstitial space separating the necrotic myofibers and showing extensive leukocyte infiltration. ETs detection appears to be markedly reduced in the DNase-I treated mice (Figure 4C). Quantitative analysis of mean fluorescent intensity (MFI) originating from ETs in the tissues, was significantly decreased in the DNase-I treated mice compared to the control group (Control: 8.23 ± 0.37 vs. DNase-I: 6.73 ± 0.50 MFI, $P = .036$, Figure-4D).

Local Markers of inflammation

Immunohistochemical analysis revealed more extensive leukocyte infiltration in the injured muscle of the control group following IR compared to DNase-I treated muscle- (Figure-5A&B). The average number of infiltrating leukocytes counted per high power field was significantly lower in the DNase-I treated group compared to control- (Control: 58.6 ± 6.8 vs. 33.2 ± 4.9 cell/hpf, $P = 0.0054$, Figure-5C). In addition, the protein levels of the CXCL1-chemokine KC was marginally higher in the DNase-I treatment group but it was not statistically significant (Control: 16.6 ± 2.1 vs. DNase-I: 22.5 ± 2.35 pg/mg Total Protein $P = .083$, Figure-5D). Similarly, the levels of the pro-inflammatory mediator MPO, revealed no difference between the two groups- (Control: 244.9 ± 16 vs. DNase-I: 238.5 ± 17.5 ng/mg Total Protein, $P = .79$, Figure-5E).

Endonuclease activity in the skeletal muscle tissue

In order to verify whether Pulmozyme treatment resulted in increased nuclease activity, we performed a plasmid incision assay on tissue extract from hind limb muscle taken from uninjured sham mice and from DNase-I treated and untreated control mice following IR (Figure-6A&B). Quantitative assessment of the relative nuclease activity shows it was markedly elevated in the control group compared to sham- (Sham: 0.75 ± 0.04 vs. Control: 1.42 ± 0.08 AU, $p < .0001$, Figure-6B). In addition, endonuclease activity was further enhanced in the DNase-I treated group compared to control (Control: 1.42 ± 0.08 vs. DNase-I: 2.26 ± 0.13 , AU, $P < .0001$, Figure-6B).

Effect of DNase-I treatment on γ -Actin protein levels in hind limb following IR

Western blot analysis shows enhanced γ -Actin detection following IR (Figure-6C). Quantitative analysis of the band densities revealed that injured skeletal muscle had markedly increased levels of γ -Actin in both the DNase-I treated and carrier buffer treated controls compared to sham- (Sham: 0.48 ± 0.18 vs. Control: 7.5 ± 2.4 vs. DNase-I: 9.2 ± 1.7 AU, $p < .01$, Figure-6D). There was no difference in the γ -Actin levels between the DNase-I treated and control group. This data suggest that IR injury enhances γ -Actin protein levels that can potentially have an inhibitory effect on DNase-I activity.

Immunofluorescent colocalization of DNase-I and γ -Actin

There was a very low level of DNase-I protein and γ -Actin proteins in the sham muscle (Figure-7 upper panels). However, in the injured muscle tissues from the mice that were treated with exogenous DNase-I (Figure-7, middle panels) or control group (Figure-7, lower panels), there was extensive DNase-I and γ -Actin detection at 24 hours following IR. Merged images demonstrated that DNase-I and γ -Actin molecules colocalized within and in the vicinity of the injured fibers in both the DNase-I treated and control groups (Figure-7, right middle and lower panels).

Effect of Neutrophil depletion on hind limb IR

To verify whether infiltrating granulocytes are responsible for the ETs formation in the injured tissue we repeated the ETs detection assay in neutrophil depleted (ND) and normal serum (NS) treated control mouse tissue. ND and NS mice had increased ETs in tissue following IR. However ND mice had significantly less ETs levels in the injured tissue suggesting that neutrophils contribute to ETs detection ($p = 0.041$, Table-I). Neutrophil depleted mice had a significantly reduced number of circulating granulocytes compared to normal serum group at 24 hours following IR ($p = .00004$, Table-I). This was accompanied by marked reduction in MPO levels in the ND mice compared to NS ($p = .0001$, Table 1). Hind limb perfusion was slightly higher in the neutrophil depleted mice compared to normal serum treated mice but this did not reach statistical significance ($p = .46$, Table-I). In addition, neutrophils depletion had no effect on muscle fiber injury ($p = .8$, Table-I) or the steady state levels of ATP ($p = .48$, Table-I). This data suggest that neutrophil depletion does not ameliorate muscle fiber morphology or indices of injury following IR.

Discussion

Administration of DNase-I in the setting of limb IR led to restoration of hind limb perfusion, decreased ETs detection, decreased leukocyte infiltration, and local markers of thrombosis (TAT III) in the injured muscle. However, DNase-I treatment neither protected against muscle fiber injury, accumulation of markers of inflammation nor improved metabolic energy sources (ATP) following acute IR. This is in contrast to studies in postischemic brain and cardiac muscle injury which found that DNase-I administration provided protection using indices of tissue viability and substantial functional recovery^{2, 14}. DNase-I treated mice had lower TAT-III levels (Figure-3D) which suggest lower incidence of thrombosis events in the tissue which also paralleled a recovery of hind limb hypoperfusion (Figure-3C) compared to control. The hypoperfusion following reperfusion injury was described as the

no-reflow-phenomenon paradox which is due to the collapsing of microvascular flow²³. While in this study, DNase-I therapy did decrease the accumulation of local markers of thrombosis and decrease postischemic hypoperfusion at 24hrs, neither of these factors could compensate for the structural (fiber injury), inflammation, or metabolic consequences of IR. To explain why these differences in skeletal muscle IR might exist, it is important to recognize that the pathophysiology of IR injury in the limb might be dramatically different from the other tissues. One important difference between these models is that both the stroke and cardiac ischemia models primarily involve arterial occlusion, whereas the limb ischemia model involves transient occlusion of both the arterial and the venous circulation which may result in compartment syndrome and more robust reperfusion injury. Immunohistochemical evaluation of postischemic skeletal muscle demonstrated extensive enhancement of ETs detected primarily in the areas of extensive muscle fiber necrosis (Figure-4). Biochemical assay of endonuclease activity in muscle tissues revealed significant increase in activity in the IR limb compared to the non-injured sham muscle (Figure-6B). Endonuclease activity was found to be exacerbated by exogenous administration of DNase-I (Figure-6B). These findings suggest that IR in skeletal muscle is associated with an increase in DNase-I expression and activity independent of exogenous sources. The addition of exogenous DNase-I treatment did not appear to provide protection against skeletal muscle IR based on the histologic or metabolic assessment. Since extensive ETs detection was observed in the location of muscle fiber necrosis despite the presence of exogenous and endogenous DNase-I, we speculate that the microenvironment of postischemic skeletal muscle might not be the optimal condition for endonuclease activity. In the tissue recycling process, the removal of cellular debris originating from dying cell is an important biological process mediated by endonucleases. DNase-I is the predominant endonuclease present in all biological fluids. In order to achieve full enzymatic activity, DNase-I requires micro-molar levels of Ca^{++} , Mg^{++} or Mn^{++} and neutral-pH. Changes in pH and ion distribution gradient in postischemic skeletal muscle may not be optimal for DNase-I activity²⁴. In fact, intracellular pH drops significantly during muscle ischemia which parallels a decrease in membrane potential and buffering capacity²⁵. Another possible explanation is that endogenous or exogenous DNase-I treatment might reduce extracellular genomic DNA but does not eliminate extracellular histones which are also known to have detrimental effects in a variety of tissue injuries²⁶⁻³⁰ including thrombosis³¹.

Another potential reason why DNase-I was not effective, can be due to the fact that its activity may be inhibited by intracellular or extracellular interaction with monomeric γ -Actin which has been described decades ago³²⁻³⁴.

This actin-DNase-I interaction, was suggested as a protective mechanism against further chromatin degradation by DNase-I influx in the injured tissue³⁵. This is also supported by findings in post-traumatic brain injury suggesting an inhibitory role of cytoskeletal actin in apoptotic cell death mediated by DNase inhibition¹⁶. Our data show that postischemic skeletal muscle has high γ -Actin content at 24hrs IR which was not altered by DNase-I treatment (Figure-6D). Analysis of the DNase activity at 24hrs following IR appears to parallel the increase in γ -Actin expression (Figure-6B&D). To provide evidence of possible DNase-I/ γ -Actin interaction, we demonstrated that γ -Actin was colocalized with DNase-I at 24 hours reperfusion using immunofluorescent microscopy (Figure-7).

To verify the potential source of ETs and γ -Actin, we analyzed hind limb skeletal muscle samples from neutrophils depleted mice and their respective normal serum treated controls following 24hrs IR for ETs and γ -Actin content. There was a slight decrease in the ETs level in the neutrophils depleted mice suggesting that neutrophil appear to be partially responsible for tissue ETs release in skeletal muscle following IR. However, successful systemic neutrophil depletion with an associated decrease in ETs neither altered hind limb perfusion nor protected against muscle necrosis following IR (Table-I). The data also revealed no difference in γ -Actin levels between the two groups suggesting that γ -Actin either leaked from the necrotic muscle fibers or released from inflammatory cells other than neutrophils (Table. I). The source of ETs is probably derived primarily from neutrophils given their cell numbers in injured tissue; however, we speculate that ETs can also originate from injured cells or as previously reported, from other inflammatory cell including, mast cells³⁶, eosinophils³⁷, and macrophages/monocytes³⁸.

Conclusions

These data suggest that while DNase-I treatment and neutrophil depletion resulted in decreased ETs levels in the injured tissue; it was not able to salvage hind limb muscle against IR injury. We speculate that the local microenvironment in injured skeletal muscle tissue contained enhanced levels of γ -Actin protein and free histones that might diminish DNase-I activity and thereby decrease its ability to provide tissue protection.

References

1. Oklu R, Albadawi H, Jones JE, Yoo HJ, Watkins MT. Reduced hind limb ischemia-reperfusion injury in Toll-like receptor-4 mutant mice is associated with decreased neutrophil extracellular traps. *J Vasc Surg.* 2013; 58:1627–36. [PubMed: 23683381]
2. Savchenko AS, Borissoff JI, Martinod K, De Meyer SF, Gallant M, Erpenbeck L, Brill A, Wang Y, Wagner DD. VWF-mediated leukocyte recruitment with chromatin decondensation by PAD4 increases myocardial ischemia/reperfusion injury in mice. *Blood.* 2014; 123:141–8. [PubMed: 24200682]
3. Liu FC, Chuang YH, Tsai YF, Yu HP. Role of neutrophil extracellular traps following injury. *Shock.* 2014; 41:491–8. [PubMed: 24837201]
4. Enzmann G, Mysiorek C, Gorina R, Cheng YJ, Ghavampour S, Hannocks MJ, Prinz V, Dirnagl U, Endres M, Prinz M, Beschorner R, Harter PN, Mittelbronn M, Engelhardt B, Sorokin L. The neurovascular unit as a selective barrier to polymorphonuclear granulocyte (PMN) infiltration into the brain after ischemic injury. *Acta neuropathologica.* 2013; 125:395–412. [PubMed: 23269317]
5. Suri R. The use of human deoxyribonuclease (rhDNase) in the management of cystic fibrosis. *BioDrugs: clinical immunotherapeutics, biopharmaceuticals and gene therapy.* 2005; 19:135–44.
6. Allen C, Thornton P, Denes A, McColl BW, Pierozynski A, Monestier M, Pinteaux E, Rothwell NJ, Allan SM. Neutrophil cerebrovascular transmigration triggers rapid neurotoxicity through release of proteases associated with decondensed DNA. *J Immunol.* 2012; 189:381–92. [PubMed: 22661091]
7. Brill A, Fuchs TA, Savchenko AS, Thomas GM, Martinod K, De Meyer SF, Bhandari AA, Wagner DD. Neutrophil extracellular traps promote deep vein thrombosis in mice. *J Thromb Haemost.* 2012; 10:136–44. [PubMed: 22044575]
8. Fuchs TA, Brill A, Duerschmied D, Schatzberg D, Monestier M, Myers DD Jr, Wroblewski SK, Wakefield TW, Hartwig JH, Wagner DD. Extracellular DNA traps promote thrombosis. *Proc Natl Acad Sci U S A.* 2010; 107:15880–5. [PubMed: 20798043]

9. Martinod K, Demers M, Fuchs TA, Wong SL, Brill A, Gallant M, Hu J, Wang Y, Wagner DD. Neutrophil histone modification by peptidylarginine deiminase 4 is critical for deep vein thrombosis in mice. *Proc Natl Acad Sci U S A*. 2013; 110:8674–9. [PubMed: 23650392]
10. Oklu R, Albadawi H, Watkins MT, Monestier M, Sillesen M, Wicky S. Detection of extracellular genomic DNA scaffold in human thrombus: implications for the use of deoxyribonuclease enzymes in thrombolysis. *Journal of vascular and interventional radiology: JVIR*. 2012; 23:712–8. [PubMed: 22525027]
11. Savchenko AS, Martinod K, Seidman MA, Wong SL, Borissoff JI, Piazza G, Libby P, Goldhaber SZ, Mitchell RN, Wagner DD. Neutrophil extracellular traps form predominantly during the organizing stage of human venous thromboembolism development. *J Thromb Haemost*. 2014
12. Oklu R, Stone JR, Albadawi H, Watkins MT. Extracellular traps in lipid-rich lesions of carotid atherosclerotic plaques: implications for lipoprotein retention and lesion progression. *Journal of vascular and interventional radiology: JVIR*. 2014; 25:631–4. [PubMed: 24581730]
13. Borissoff JI, Joosen IA, Versteylen MO, Brill A, Fuchs TA, Savchenko AS, Gallant M, Martinod K, Ten Cate H, Hofstra L, Crijns HJ, Wagner DD, Kietselaer BL. Elevated levels of circulating DNA and chromatin are independently associated with severe coronary atherosclerosis and a prothrombotic state. *Arterioscler Thromb Vasc Biol*. 2013; 33:2032–40. [PubMed: 23818485]
14. De Meyer SF, Suidan GL, Fuchs TA, Monestier M, Wagner DD. Extracellular chromatin is an important mediator of ischemic stroke in mice. *Arterioscler Thromb Vasc Biol*. 2012; 32:1884–91. [PubMed: 22628431]
15. Snabes MC, Boyd AE 3rd, Pardue RL, Bryan J. A DNase I binding/immunoprecipitation assay for actin. *The Journal of biological chemistry*. 1981; 256:6291–5. [PubMed: 6263912]
16. Bareyre FM, Raghupathi R, Saatman KE, McIntosh TK. DNase I disinhibition is predominantly associated with actin hyperpolymerization after traumatic brain injury. *Journal of neurochemistry*. 2001; 77:173–81. [PubMed: 11279273]
17. Crawford RS, Hashmi FF, Jones JE, Albadawi H, McCormack M, Eberlin K, Entabi F, Atkins MD, Conrad MF, Austen WG Jr, Watkins MT. A novel model of acute murine hindlimb ischemia. *American journal of physiology Heart and circulatory physiology*. 2007; 292:H830–7. [PubMed: 17012358]
18. McCormack MC, Kwon E, Eberlin KR, Randolph M, Friend DS, Thomas AC, Watkins MT, Austen WG Jr. Development of reproducible histologic injury severity scores: skeletal muscle reperfusion injury. *Surgery*. 2008; 143:126–33. [PubMed: 18154940]
19. Albadawi H, Oklu R, Cormier NR, O'Keefe RM, Heaton JT, Kobler JB, Austen WG, Watkins MT. Hind limb ischemia-reperfusion injury in diet-induced obese mice. *J Surg Res*. 2014
20. Buzder T, Yin X, Wang X, Banfalvi G, Basnakian AG. Uptake of foreign nucleic acids in kidney tubular epithelial cells deficient in proapoptotic endonucleases. *DNA Cell Biol*. 2009; 28:435–42. [PubMed: 19558214]
21. Basnakian AG, Ueda N, Kaushal GP, Mikhailova MV, Shah SV. DNase I-like endonuclease in rat kidney cortex that is activated during ischemia/reperfusion injury. *J Am Soc Nephrol*. 2002; 13:1000–7. [PubMed: 11912259]
22. Romero-Calvo I, Ocon B, Martinez-Moya P, Suarez MD, Zarzuelo A, Martinez-Augustin O, de Medina FS. Reversible Ponceau staining as a loading control alternative to actin in Western blots. *Analytical biochemistry*. 2010; 401:318–20. [PubMed: 20206115]
23. Blaisdell FW. The pathophysiology of skeletal muscle ischemia and the reperfusion syndrome: a review. *Cardiovascular surgery*. 2002; 10:620–30. [PubMed: 12453699]
24. Yao M, Keogh A, Spratt P, dos Remedios CG, Kiessling PC. Elevated DNase I levels in human idiopathic dilated cardiomyopathy: an indicator of apoptosis? *Journal of molecular and cellular cardiology*. 1996; 28:95–101. [PubMed: 8745217]
25. Hagberg H. Intracellular pH during ischemia in skeletal muscle: relationship to membrane potential, extracellular pH, tissue lactic acid and ATP. *Pflugers Archiv: European journal of physiology*. 1985; 404:342–7. [PubMed: 4059028]
26. Wildhagen KC, Garcia de Frutos P, Reutelingsperger CP, Schrijver R, Areste C, Ortega-Gomez A, Deckers NM, Hemker HC, Soehnlein O, Nicolaes GA. Nonanticoagulant heparin prevents histone-

- mediated cytotoxicity in vitro and improves survival in sepsis. *Blood*. 2014; 123:1098–101. [PubMed: 24264231]
27. Pisetsky DS. Immune activation by histones: pluses and minuses in inflammation. *European journal of immunology*. 2013; 43:3163–6. [PubMed: 24165954]
 28. Allam R, Darisipudi MN, Tschopp J, Anders HJ. Histones trigger sterile inflammation by activating the NLRP3 inflammasome. *European journal of immunology*. 2013; 43:3336–42. [PubMed: 23964013]
 29. Xu J, Zhang X, Monestier M, Esmon NL, Esmon CT. Extracellular histones are mediators of death through TLR2 and TLR4 in mouse fatal liver injury. *J Immunol*. 2011; 187:2626–31. [PubMed: 21784973]
 30. Allam R, Kumar SV, Darisipudi MN, Anders HJ. Extracellular histones in tissue injury and inflammation. *J Mol Med (Berl)*. 2014; 92:465–72. [PubMed: 24706102]
 31. Lam FW, Cruz MA, Leung HC, Parikh KS, Smith CW, Rumbaut RE. Histone induced platelet aggregation is inhibited by normal albumin. *Thrombosis research*. 2013; 132:69–76. [PubMed: 23673386]
 32. Macanovic M, Lachmann PJ. Measurement of deoxyribonuclease I (DNase) in the serum and urine of systemic lupus erythematosus (SLE)-prone NZB/NZW mice by a new radial enzyme diffusion assay. *Clin Exp Immunol*. 1997; 108:220–6. [PubMed: 9158089]
 33. Malicka-Blaszkiewicz M. Rat liver DNase I-like activity and its interaction with actin. *Zeitschrift fur Naturforschung C, Journal of biosciences*. 1990; 45:1165–70. [PubMed: 2095786]
 34. Mannherz HG, Goody RS, Konrad M, Nowak E. The interaction of bovine pancreatic deoxyribonuclease I and skeletal muscle actin. *European journal of biochemistry/FEBS*. 1980; 104:367–79. [PubMed: 6244947]
 35. Eulitz D, Mannherz HG. Inhibition of deoxyribonuclease I by actin is to protect cells from premature cell death. *Apoptosis: an international journal on programmed cell death*. 2007; 12:1511–21. [PubMed: 17468836]
 36. von Kockritz-Blickwede M, Goldmann O, Thulin P, Heinemann K, Norrby-Teglund A, Rohde M, Medina E. Phagocytosis-independent antimicrobial activity of mast cells by means of extracellular trap formation. *Blood*. 2008; 111:3070–80. [PubMed: 18182576]
 37. Yousefi S, Gold JA, Andina N, Lee JJ, Kelly AM, Kozlowski E, Schmid I, Straumann A, Reichenbach J, Gleich GJ, Simon HU. Catapult-like release of mitochondrial DNA by eosinophils contributes to antibacterial defense. *Nature medicine*. 2008; 14:949–53.
 38. Chow OA, von Kockritz-Blickwede M, Bright AT, Hensler ME, Zinkernagel AS, Cogen AL, Gallo RL, Monestier M, Wang Y, Glass CK, Nizet V. Statins enhance formation of phagocyte extracellular traps. *Cell host & microbe*. 2010; 8:445–54. [PubMed: 21075355]

Clinical Relevance

Acute muscle ischemia-reperfusion injury following traumatic event or thrombotic occlusion of a major artery due to vascular disease in the lower extremities can lead to extensive tissue inflammation and necrosis. Recently, DNase-I was proposed as a treatment strategy to degrade neutrophil extracellular traps which consist of protein-DNA complexes accumulating after tissue injury or thrombosis. Investigators believe that these complexes can enhance the prothrombotic and proinflammatory milieu in the tissue, thereby exacerbating injury. In this study, we investigate the benefit of DNase-I treatment as a tool to degrade these complexes aiming to ameliorate muscle ischemia-reperfusion injury.

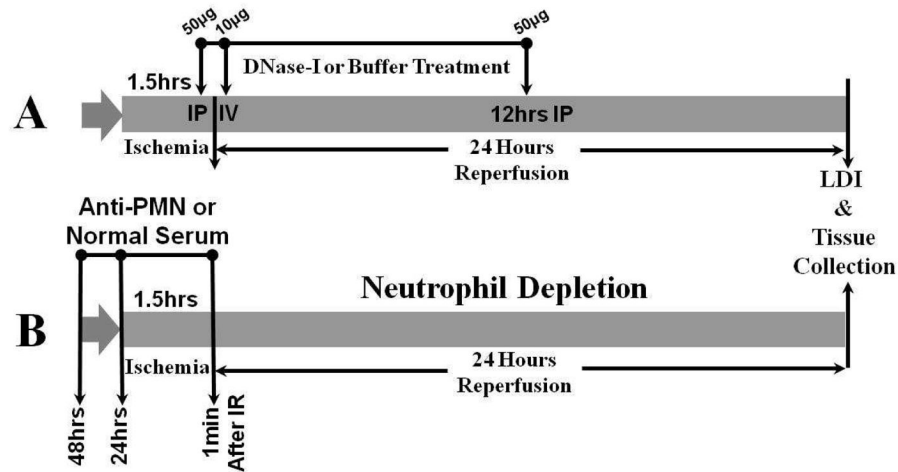


Figure 1. Schematic diagram of acute hind limb ischemia reperfusion and treatment protocols C57BL6 male mice were subjected to 1.5 hours of unilateral hind limb tourniquet ischemia followed by 24 hours reperfusion. In the first set of experiments (diagram A), mice were subjected to IR and split into two groups. The first group received 50 µg of human recombinant DNase-I (Pulmozyme, n=8) intraperitoneally at 5 minutes before reperfusion and a second dose of 10µg intravenously at 10 minutes after reperfusion and a third dose of 50µg intraperitoneally at 12 hours after reperfusion. The second control group received similar volumes of carrier buffer alone at the same time points (n=8). In the second part of this study (diagram B), two separate groups of mice received daily injections of either rabbit anti-mouse neutrophil serum intraperitoneally for neutrophil depletion (n=8), or normal rabbit serum (n=7) for 48hrs two days prior to IR. Mice were then subjected to 1.5hrs unilateral ischemia IR injury and received additional rabbit anti-mouse serum or normal serum 1 minute after the start of reperfusion. AT the end of 24 hours IR period, hind limb perfusion was documented with a laser Doppler imaging, then mice were euthanized and hind limb muscle tissues were harvested for analysis.

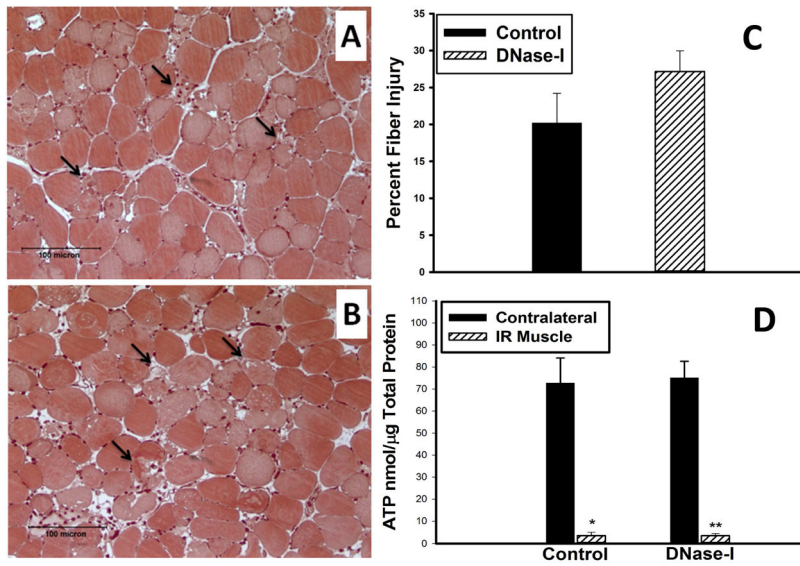


Figure 2. Effect of DNase-I treatment on muscle fiber injury and ATP levels following acute IR. Image A and B, are representative micrographs of Mason’s trichrome stained acrylic imbedded TA muscle shows the muscle tissue morphology in cross sections following IR from control (A) and DNase-I treated (B) mice. Injured muscle fibers are evident in the field such as the one indicated by black arrow with observed edema, hemorrhage, and leukocytes infiltration. Quantitative analysis of the percent muscle fiber injury per randomized per high power field is summarized in the graph (C), and muscle ATP summarized in the graph (D) revealed that, DNase-1 treatment did not alter skeletal muscle fiber injury or the steady state levels of ATP.

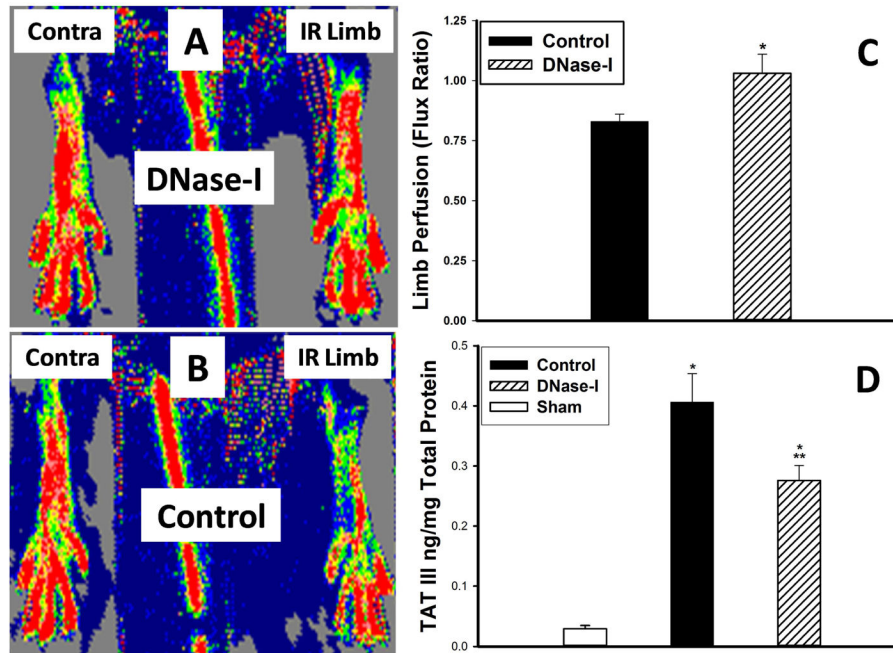


Figure 3.

Effect of DNase-I treatment on hind limb perfusion and TAT III levels in the hind limb muscle following IR. The Laser Doppler scanner generated images (A&B) demonstrates the degree of perfusion in each hind limb (red to be the highest perfusion in contrast to dark blue which represent no perfusion). The IR limb in the Pulmozyme treated mouse (Figure-2A) appear to have similar perfusion compared to the uninjured contralateral limb while the IR limb in the untreated control mice (Figure-2B) have diminished perfusion compared to the contralateral limb. Calculating the hind limbs the scanner generated Flux ratio the hind limbs in each mouse as an index of limb perfusion revealed, significantly higher perfusion at 24 hours reperfusion in the DNase-I treated mice compared to the control group (* $p=0.02$, C). Hind limb tissue TAT III levels significantly increased following IR in both control and the DNase-I treated group compared to sham (* $p<0.001$). However the TAT III levels were significantly lower in the DNase-I treated mice compared to control (** $p<0.05$). This data suggest that DNase-I treatment ameliorated tissue thrombosis which paralleled higher hind limb perfusion.

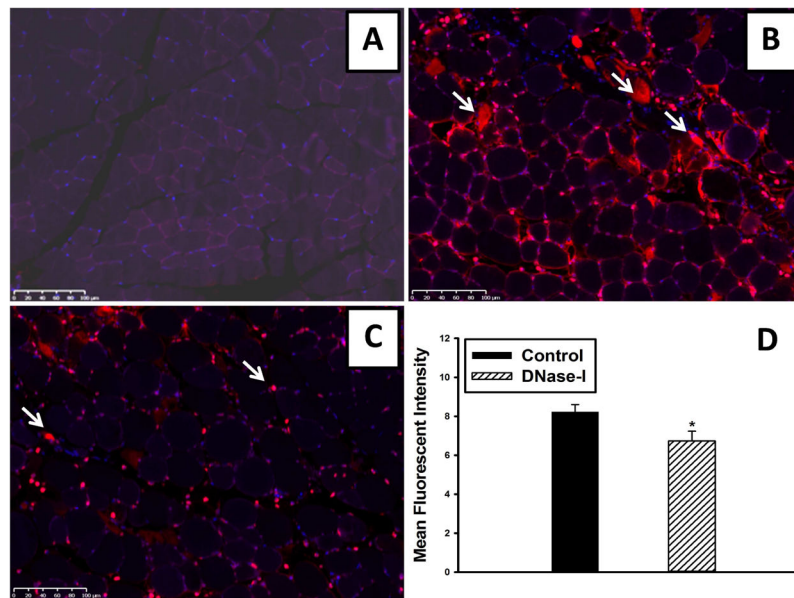


Figure 4. Effect of DNase-I treatment on ETs detection following IR. Representative images from Cy3 labeled ETs immunostaining. ETs were not detectable in the non-injured sham muscle (A). However, there was extensive ETs detection observed in the interstitium of the injured muscle fibers as indicated by white arrows (B). DNase-I treatment significantly reduced ETs detection in the tissue following IR (C). Mean fluorescent intensity values for DNase-I treated and untreated control mice are summarized in the graph (* $p=.036$, D).

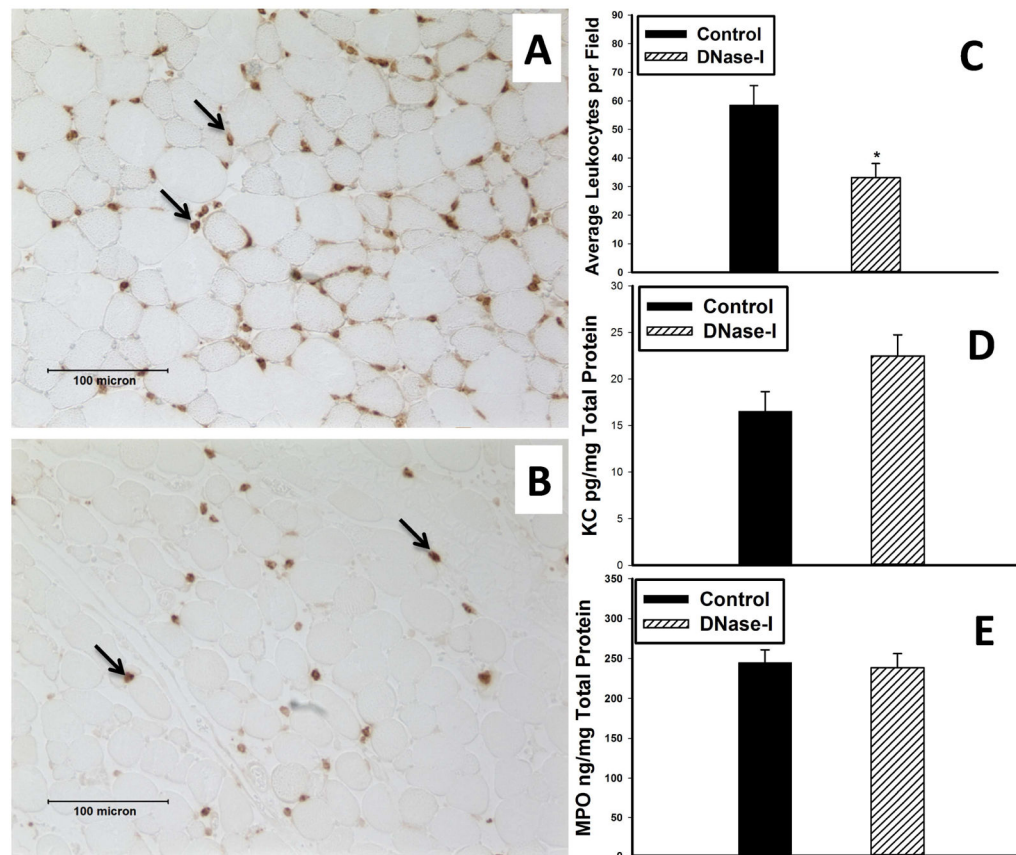


Figure 5.

Effect of DNase-I treatment on muscle inflammation following IR. Left Images A and B, are representative micrographs of TA muscle demonstrate immunostaining for the leukocytes marker-Ly6B (brown color) in the tissue sections following IR obtained from control (A) or DNase-I treated (B) mice. Quantitative analysis of Ly6B positive cells count, KC and MPO levels are summarized in the graphs, revealed that DNase-I treatment markedly reduced the average number of leukocytes (*P=0.0054, C) but did not alter skeletal muscle KC (D) or MPO (E) levels at 24 hours following IR.

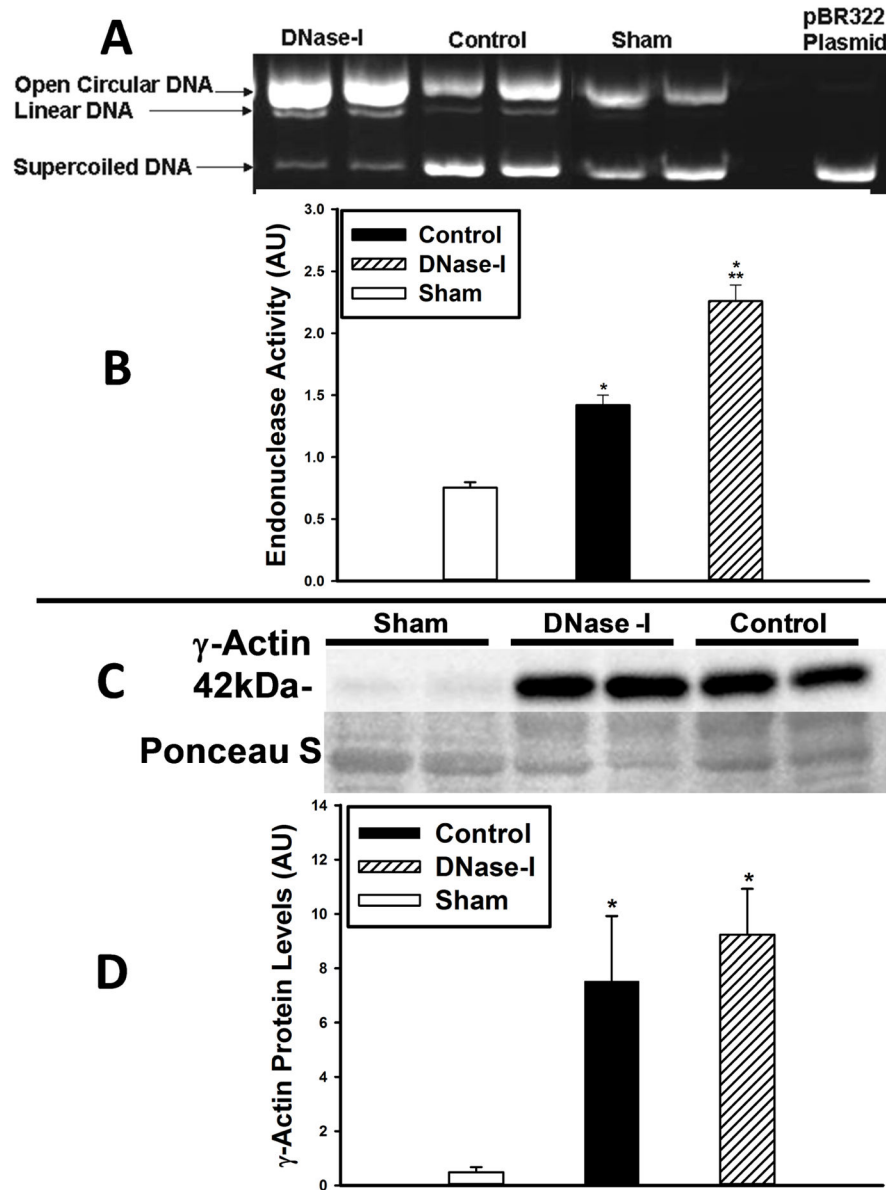


Figure 6.

Effect of DNase-I treatment of endonuclease activity and γ -Actin protein levels following IR. Endonuclease activity was evaluated with plasmid incision assay in skeletal muscle tissue protein extracts from sham, DNase-I treated and untreated control mice (A&B). The representative image (A) show the bands for the open circular and linear forms of the plasmid DNA which increased over the supercoiled DNA in the DNase-I treated and control groups compared to sham indicating increased endonuclease activity while the right lane of the gel image represent the pBR322 plasmid alone which only present a supercoiled plasmid DNA form. Quantitative analysis (B) shows that endonuclease activity was markedly elevated in both the control and DNase-I treated groups over sham levels (* $P < 0.01$, B) with significantly higher levels detected in the DNase-I group compared to control (** $P < .05$, B). This data suggest that DNase-I treatment further enhanced endonuclease activity following

IR. Analysis of γ -Actin protein expression by western blotting, shows an enhanced γ -Actin protein expression following IRas compared to sham (C). Quantitative analysis of the 42kDa γ -Actin band densities normalized to the Poncaue-S bands are displayed in the summary graph (D). Data shows a significant increase γ -Actin protein in the post ischemic hind limb muscle in the DNase-I treated and control groups compared to sham (* $p < .01$, D). There was no difference in the γ -Actin levels between the DNase-I treated and control groups (D). This data suggest that DNase-I treatment did not alter the γ -Actin protein levels.

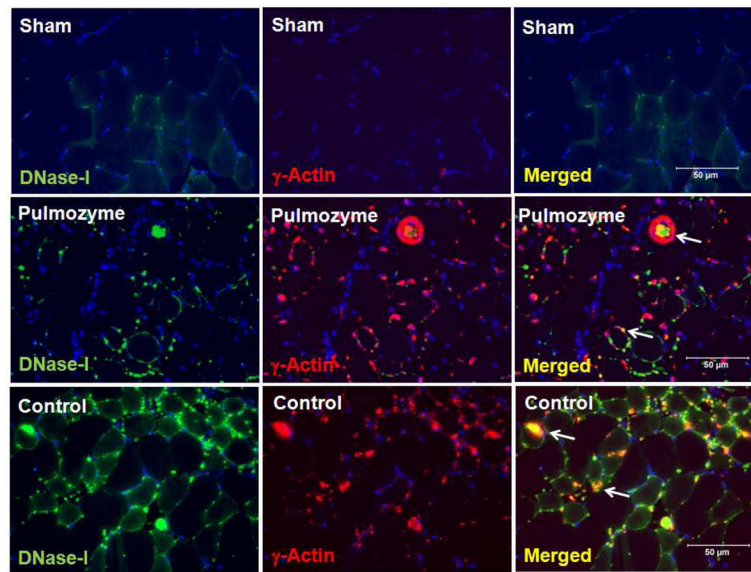


Figure 7. Immunofluorescence localization of DNase-I with γ -Actin proteins in skeletal muscle tissue following IR with and without exogenous DNase-I treatment. Images in the panel are representative of dual immunofluorescence detection of DNase-I and γ -Actin using Alexa-488 and Cy3 fluorochrome conjugated secondary IgG respectively in skeletal muscle tissue from uninjured sham hind limb and following IR. In the sham mice (top images), there was very low level of DNase-I (top left, green) or γ -Actin (top left middle, red) and merged (top right), detected in the tissue. However, we observed in the mice that were treated with DNase-I (Pulmozyme, middle images) or in the control group (lower images) extensive DNase-I (Green color) and γ -Actin (Red color) staining detected at 24 hours following IR. Merged fluorescent images demonstrated that DNase-I and γ -Actin molecules colocalized within and around the injured fibers in the DNase-I treated and control groups (merged colors in yellow/Orange). The colocaliation of DNase-I suggest that DNase-I might be inhibited in the presence of γ -Actin in the injured tissue.

Table I

Data summary of the effect of neutrophil depletion on hind limb skeletal muscle after IR. Tissues from mice treated with anti-Neutrophil serum (ND) or normal serum (NS) were harvested 24 hours following IR. Neutrophil depletion significantly decreased plasma levels of circulating granulocytes (*) together with reduced MPO (†) and ETs (‡) in the injured tissue. However, Neutrophil depletion did not significantly alter hind limb perfusion, muscle fiber injury, the steady state level of ATP or γ -Actin protein levels. *, †, ‡ indicates significant difference from the normal serum group.

	Neutrophil Depleted (ND)	Normal Serum (NS)	P value
Granulocytes $10^3/\mu\text{l}$	0.14 \pm 0.02	1.11 \pm 0.15	*0.00004
MPO ng/mg	63.5 \pm 15.8	261.6 \pm 14.7	†0.0001
ETs (MFI)	11.6 \pm 0.5	15 \pm 1.7	‡0.041
Perfusion Ratio	1.128 \pm 0.232	0.848 \pm 0.097	0.46
% Injured Fibers	30.76 \pm 1.97	29.68 \pm 1	0.8
ATP nmole/ μg protein	0.42 \pm 0.22	0.74 \pm 0.3	0.48
γ -Actin protein levels (AU)	2.5 \pm 0.54	3.56 \pm 0.78	0.25